


Sustainable development substantially reduces the risk of future drought impacts

Hossein Tabari ^{1,2,3}✉ & Patrick Willems¹

Drought is a major natural hazard that can cause cascading impacts on socioeconomic sectors, and its risk is expected to increase under future climate change and socioeconomic developments. However, a comprehensive cross-disciplinary drought risk outlook is currently lacking to support integrative disaster risk reduction efforts. To address this gap, our analysis examines drought exposure, vulnerability, and risk towards the end of this century under four future pathways. The study identifies the Mediterranean, Amazon, southern Africa, and Central America as the most impacted regions where extreme multivariate drought is projected to become two to four times more likely. Our analysis also shows that sustainable development would reduce population exposure to drought by 70% compared to fossil-fueled development. Furthermore, it halves the number of countries facing a fivefold increase in drought risk. Our results underscore the critical need for a cross-disciplinary drought risk outlook and emphasize the importance of considering exposure and vulnerability for risk assessments.

¹Department of Civil Engineering, KU Leuven, Leuven, Belgium. ²Department of Meteorological and Climate Research, Royal Meteorological Institute of Belgium, Uccle, Belgium. ³Faculty of Applied Engineering, University of Antwerp, Antwerp, Belgium. ✉email: hossein.tabari@uantwerpen.be

Drought is a major natural hazard worldwide, given its prevalence over the past few decades in various regions, such as Australia during 1997–2009, southwest China during 2009–2010, eastern Africa during 2010–2012, and the Middle East during 1998–2012. Drought has caused massive damages, accounting for 34% of disaster-related deaths between 1970 and 2019¹. Its risk as a function of hazard, exposure, and vulnerability is also expected to amplify under future climatic and socioeconomic changes^{2–4}. Recognizing the importance of understanding drought and assessing proactive measures to mitigate its disaster risk, the High-Level Meeting on National Drought Policies (HMNDP) in March 2013 emphasized the necessity of this task⁵. To achieve the Sustainable Development Goals (SDGs) by 2030, reducing risk and strengthening society's drought resilience was also acknowledged as an important task⁶.

Drought is a complex hazard that encompasses a series of interactive physical processes and can cause cascading impacts on different socioeconomic sectors^{7,8}. Drought risk assessment for one sector, such as agriculture, cannot be generalized for another sector that requires a different physical form of drought, such as hydrological or meteorological. Each drought index considers specific hydroclimate processes⁹, and a meteorological drought, which refers to a precipitation deficit, does not necessarily propagate to an agricultural drought, which refers to a soil moisture deficit, especially in regions with relatively high average precipitation¹⁰. Furthermore, future global warming is expected to cause a more widespread and intense drying signal for soil moisture and runoff^{11,12}, compared to highly uncertain precipitation responses in many regions and seasons¹³. The projected larger changes in soil moisture and runoff highlight the importance of non-precipitation processes such as increased evaporative demand in the atmosphere^{14,15} and vegetation water use¹⁶ for agricultural and hydrological droughts. Failing to adequately account for the needs of end-users in different sectors and disregarding the low intersubstitutability of drought results from one domain to another¹⁷ can lead to blind spots in risk mitigation and adaptation planning. To avoid this happening, a multivariate drought assessment is required through the analysis of multiple hydroclimatic variables to represent broad responses of the entire hydrological cycle to climatic and socioeconomic changes. While several studies have been conducted using multivariate indices to analyze future drought at small scales^{7,18,19}, global studies have mainly focused on historical periods^{20,21}, and there is a lack of global assessments of future multivariate drought risk that account for hazard, exposure, and vulnerability.

Previous global drought risk assessments have quantified the risk of only one type of drought at a time^{15,22}. However, quantifying univariate drought may not be reliable for comprehensive regional integrated management of drought risk^{23,24}. In the few existing univariate global drought risk studies, exposure and/or vulnerability were disregarded or assumed constant over time^{4,25–30}. A static assumption for exposure and/or vulnerability, however, is a serious limitation in risk estimates, as the three components of risk are subject to change over time through geomorphologic, socioeconomic, and climate influences^{31–34}. In this context, future population growth in hazard-prone areas was found to be an even more important factor than hazard amplification for the future risk increase of some extreme events³⁵.

To address these shortcomings, we perform a future (late 21st century) risk analysis of multivariate droughts which integrates the drought information from precipitation (meteorological), runoff (hydrological), and soil moisture (agricultural) using the joint distribution function of the three variables (see Methods). The drought risk is derived as the product of the occurrence probability of drought (hazard), population exposure, and the Human Development Index (HDI)³⁶ as an indicator of

vulnerability. Since in vulnerable societies dire impacts are not always resulted from the most extreme events³⁷, the risk analysis is conducted for three extremity levels of drought including moderate, severe, and extreme. The changes in the multivariate drought risk are projected towards the end of this century under four Shared Socioeconomic Pathways (SSPs)³⁸ and then decomposed into hazard, exposure, and vulnerability contributions to assess the drivers of risk changes.

Results

The analysis of climate change impacts on annual (12-month) droughts shows that the probability of drought occurrence is increasing (probability ratio >1) in many parts of the world based on the ensemble median (Fig. 1). However, there is considerable uncertainty in the sign of projected changes in drought probability in many global regions. Regions such as South America, Central America, Australia, the Mediterranean, southern Africa, southeastern Asia, and North America are projected to experience a rise in drought probability in the late 21st century relative to the historical period (1971–2000). The increase in hazard probability is robust, especially for high emission and socioeconomic scenarios, in all these regions except for Australia and parts of southern Africa and southeastern Asia. In these regions, the magnitude of the increase in drought probability is proportional to the severity of droughts, with extreme droughts experiencing the largest increase. Climate change impact is also expected to rise with the increase in emissions and socioeconomic scenarios.

On the other hand, some regions are expected to experience a decrease in the probability of droughts. A robust decrease is mainly found in central Africa and most of southern Asia. The analysis for 3-month droughts shows a similar spatial pattern and magnitude of changes in drought probability, but with slightly lower values (Supplementary Fig. 1). The results for a 12-month scale are hereafter presented and discussed in the paper.

Regions such as the Mediterranean, Amazon, southern Africa, and Central America (see Supplementary Fig. 2 for the defined domain for these regions) are identified as hotspots with the worst climate change impact on future droughts. For instance, the Mediterranean is projected to experience an increase of 2.5, 3.3, 4, and 4.4 times more frequent extreme droughts under the SSP1, SSP2, SSP3, and SSP5 scenarios, respectively (Fig. 2). The increase is smaller for less extreme drought events. For the SSP1, SSP2, SSP3, and SSP5 scenarios, respectively, 1.9, 2.3, 2.9, and 3.1 times more frequent severe droughts are expected to occur by the end of this century for the Mediterranean region (Supplementary Fig. 3) and 1.6, 1.7, 2.1, and 2.2 times more frequent moderate droughts (Supplementary Fig. 4). Similarly, Central America and Amazon are expected to experience a similar pattern to the Mediterranean, but with smaller drought probability amplification. The future extreme drought probability in Central America shows 1.7-, 2.2-, 2.8-, and 3.1-fold increases for the respective scenarios (Fig. 2). The drought probability is projected to become between 1.5 (SSP1) and 2.5 (SSP5) times larger for severe droughts and between 1.3 (SSP1) and 1.9 (SSP5) times larger for moderate droughts (Supplementary Figs. 3, 4). In Amazon, the occurrence probability of extreme droughts gets 1.6, 1.9, 2.6, and 2.7 times larger in the future for SSP1, SSP2, SSP3, and SSP5, respectively (Fig. 2). The occurrence probability rises between 1.4-fold (SSP1) and 2.1-fold (SSP5) for severe drought and between 1.3-fold (SSP1) and 1.7-fold (SSP5) for moderate drought in Amazon (Supplementary Figs. 3, 4). Southern Africa is also projected to see an increase of 1.6, 2, 2.2, and 2.4 times larger probabilities of extreme droughts under SSP1, SSP2, SSP3, and SSP5, respectively (Fig. 2). For the respective scenarios, 1.4-, 1.5-, 1.7-, and 1.8-fold increases for severe droughts and 1.3-, 1.4-, 1.5-,

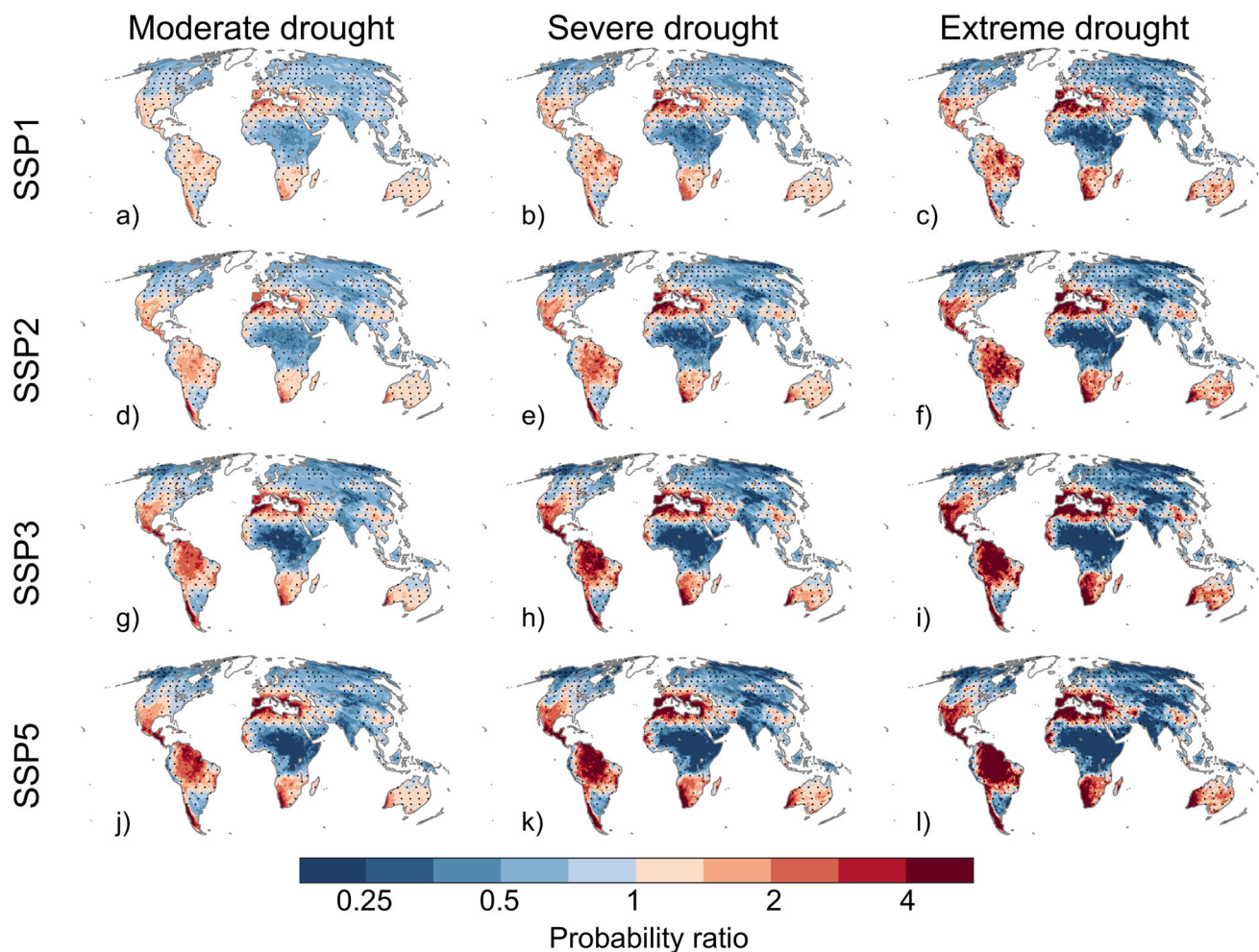


Fig. 1 Drought probability ratio between the late 20th century and the late 21st century. The ratio of the occurrence probability of moderate (a, d, g, j), severe (b, e, h, k), and extreme (c, f, i, l) droughts for a 12-month scale based on the CMIP6 multi-model median by the late 21st century (2070–2099) under different scenarios to the historical baseline period (1971–2000). Stippling indicates areas where fewer than 72% of models (13 out of the 18 GCMs) agree on the sign of the probability ratio. See Supplementary Fig. 1 for the drought probability ratio of a 3-month scale.

and 1.5-fold increases for moderate droughts are expected in southern Africa (Supplementary Figs. 3, 4).

Projected changes in the occurrence probability of droughts, along with changes in population density, influence the number of people exposed to the hazard. For all extremity levels of droughts (moderate, severe, and extreme), the highest population exposure is found for the SSP3 scenario (Fig. 3 and Supplementary Figs. 5, 6), due to the highest projected population (Supplementary Fig. 7) and a large increase in drought occurrence probability (Fig. 1). The highest population exposure for SSP3 is also seen for the hotspot regions. The global population exposure to droughts under SSP3 is 70% higher than that under SSP1. The population exposure also increases with drought extremity and reaches ~130% of the present global population for extreme droughts under SSP3. The GCM uncertainty is also shown in Fig. 3 and Supplementary Figs. 5, 6, which increases with drought extremity.

To take into account vulnerability for deriving future drought risk, the Human Development Index (HDI) for historical and future periods (Supplementary Fig. 8) was used as a proxy of vulnerability and integrated with the country-level drought hazard (Supplementary Figs. 9, 10) and population. Comparing Fig. 4 and Supplementary Fig. 10 reveals the importance of exposure and vulnerability in shaping the future perspective of drought risk. The number of countries facing a fivefold risk

increase approximately doubles from SSP1 to SSP5; from 11–13 countries to 22–25 countries (Fig. 4 and see Supplementary Fig. 11 for drought risk factors when hazard, exposure, and vulnerability are not normalized). The highest increases in drought risk are mostly projected for the Mediterranean countries, including Portugal, Spain, Greece, Macedonia, Jordan, Israel, and Syria. Guatemala, Chile, Zambia, and Madagascar are also projected to experience a very large increase in drought risk.

In order to understand the underlying factors contributing to the substantial increases in drought risk, this study conducted a decomposition analysis of risk, looking at the roles of hazard, exposure, and vulnerability. The results showed that, for both countries with increasing and decreasing risk, hazard was the main driver of risk for all drought extremity levels and future scenarios, except for a moderate decrease in risk under SSP3, where exposure played a larger role (Fig. 5). Specifically, hazard accounted for 37–78% of the change in risk, and this contribution was generally greater for decreasing risk cases and for more extreme droughts. The contribution of hazard is mostly larger for decreasing risk cases compared to increasing ones and it rises with drought extremity. On the other hand, the contribution of exposure and vulnerability to future drought risk was generally larger for countries experiencing an increased risk compared to those with a decreasing risk. However, it's important to note that the vulnerability index used in this analysis was not specifically

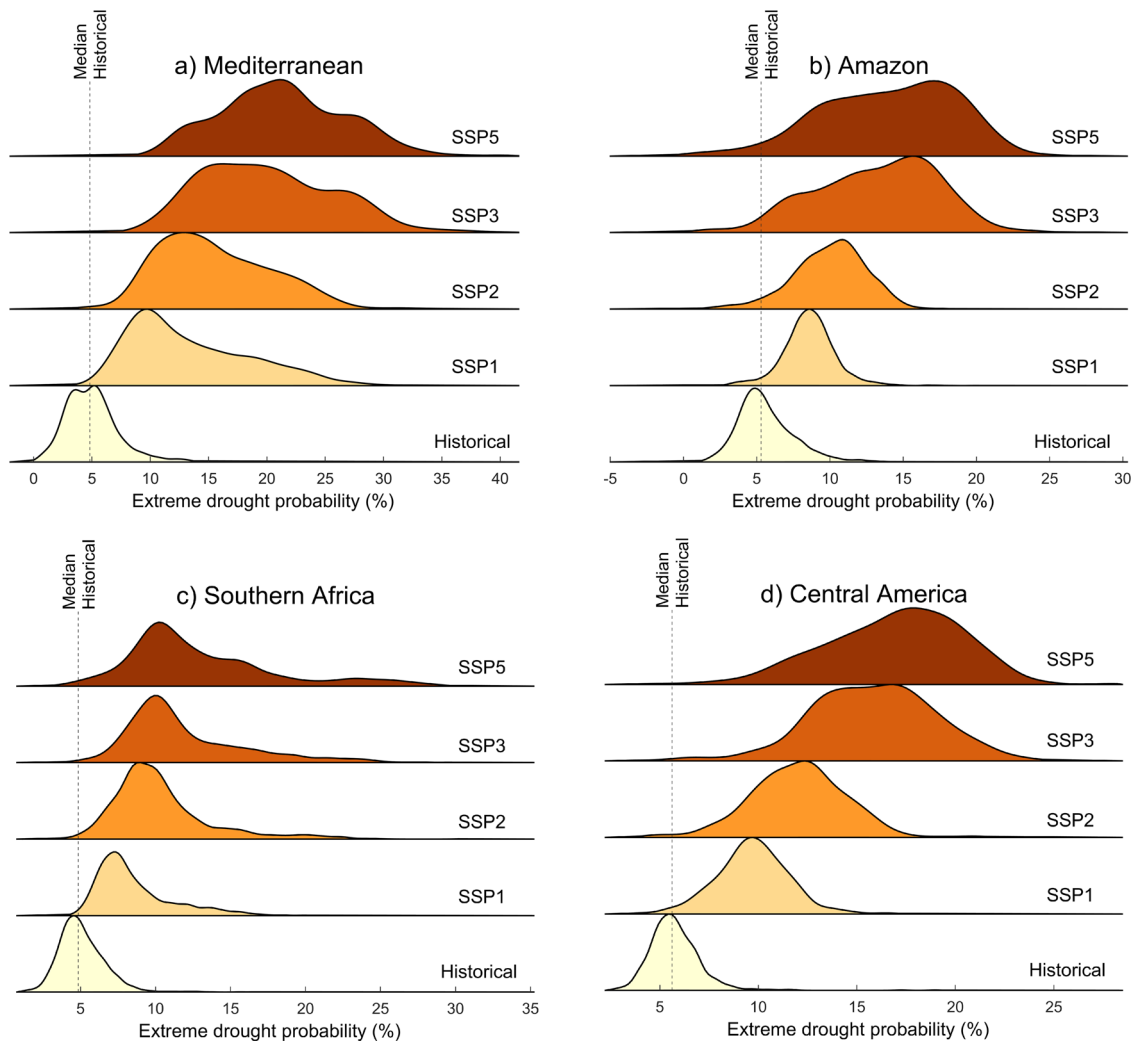


Fig. 2 Distribution functions of extreme drought probability based on the CMIP6 multi-model median in the grid cells of hotspot regions for the historical period (1971–2000) and the late 21st century (2070–2099) under different scenarios. The results are shown for the annual (12-month) scale for the Mediterranean (a), Amazon (b), Southern Africa (c), and Central America (d). The median probability for the baseline period as the reference is shown by the vertical dashed line. See Supplementary Figs. 3, 4 for the distribution functions of severe and moderate drought probabilities, respectively.

developed for drought, and using a more drought-tailored vulnerability index may provide a more accurate estimation of the vulnerability contribution to future drought risk. Overall, this decomposition analysis provides insight into the complex interplay of different factors driving drought risk and highlights the need for tailored approaches to address and mitigate the impacts of drought in different regions.

Discussion

This study provided a multi-sectoral outlook of future drought risk towards the end of this century under four SSP scenarios. The multivariate droughts integrated the drought information from precipitation, runoff, and soil moisture. The drought risk was derived as a function of the occurrence probability of moderate, severe, and extreme droughts, population exposure, and the Human Development Index (HDI) as a proxy for vulnerability. In addition, the drivers of drought risk were explored by decomposing the changes into the contributions of the three risk components, including hazard, exposure, and vulnerability.

The results indicate that climate change is likely to increase the probability of droughts in many parts of the world, particularly in vulnerable regions such as South America, Central America, Australia, the Mediterranean region, and southern Africa. The

Mediterranean, Amazon, southern Africa, and Central America are the most impacted regions where extreme drought probability is projected to become between 1.6 and 4.4 times larger, depending on the SSP scenario. The large increase in drought occurrence could substantially increase drought damage in vulnerable societies, especially in the regions where people are dependent on farming for their livelihoods (poor people in rural areas of developing countries³⁹) and lack financial, technological, and institutional resources to cope with the consequences of droughts⁴⁰.

We also find that more extreme drought events are associated with a larger increase in the probability of drought. This trend is consistent with other types of extreme events, such as extreme temperatures, precipitation, and flooding, which have also been shown to have a larger climate change signal for more extreme events^{41–45}. Our results further highlight that the impact of climate change on drought probability is expected to increase with the SSP scenario as expected⁴⁶. Global warming at the end of this century compared to the current climate based on the CMIP6 ensemble mean ranges from 0.69 °C for SSP1 to 3.99 °C for SSP5⁴⁷. The higher the warming, the larger the change in the climate, with evaporation as one of the key variables influencing drought expected to increase at a rate of 1.5–4% per degree of warming⁴⁸.

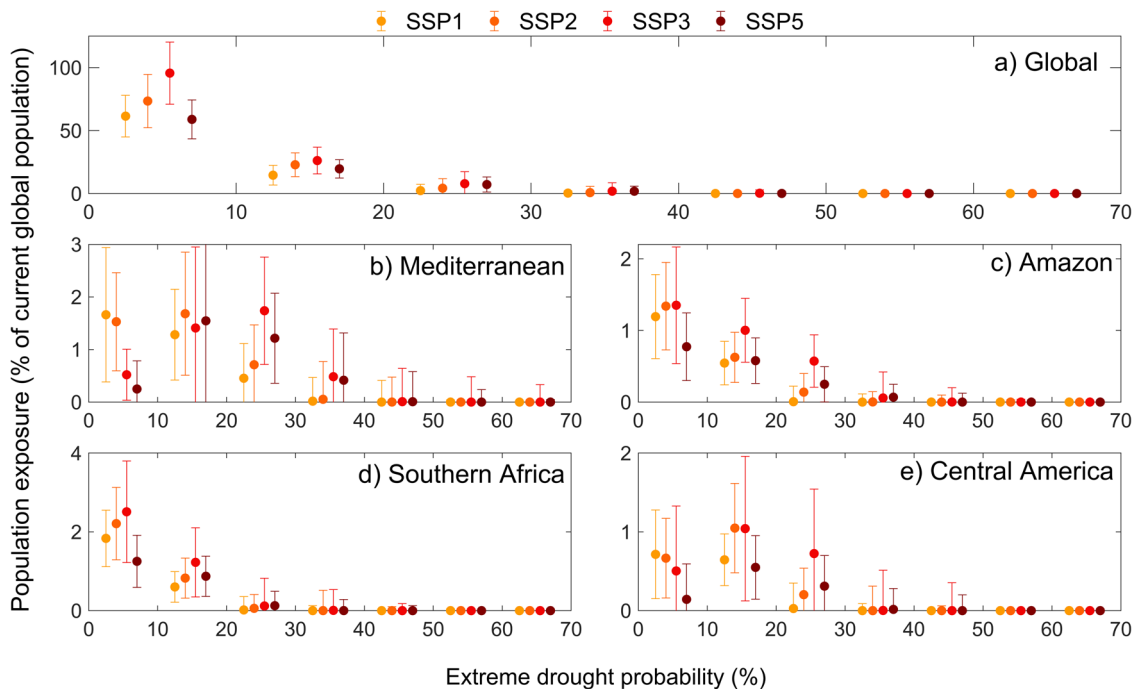


Fig. 3 Population exposure to extreme droughts during the late 21st century period. Population exposure to different probabilities of extreme drought events at a 12-month scale occurring during the late 21st century period (2070–2099) under different scenarios by individual GCMs at the global scale (a) and in the Mediterranean (b), Amazon (c), Southern Africa (d), and Central America (e). Circle and error bars represent the CMIP6 multi-model ensemble median and standard deviation (GCM uncertainty), respectively. The exposed population is expressed as a percentage of the current global population. See Supplementary Figs. 5, 6 for the population exposure to severe and moderate drought probabilities, respectively.

Results suggest that population exposure to droughts is projected to be the highest under the SSP3 scenario due to a combination of two factors: a high probability of drought occurrence and a large projected population because of relatively low investments in human capital. In contrast, the population exposure to droughts is projected to be the lowest under the SSP1 scenario, which is characterized by sustainable development and strong investments in human capital. The estimated population exposure under SSP1 is globally 70% lower than that under SSP3, highlighting the importance of investments in human capital and sustainable development for reducing drought impacts. This indicates that the magnitude of population exposure to droughts in the future will depend not only on the climate change scenario but also on how socioeconomic factors such as population growth and human capital investment evolve.

The results of this work indicate that some parts of the world are expected to face unprecedented increases in drought risk, whose magnitudes depend strongly on future emissions and socioeconomic pathways. The analysis highlights the largest drought risk changes for SSP5 when the number of countries facing a fivefold risk intensification is twice as large as that for SSP1; 22–25 countries versus 11–13 countries. A higher drought risk as the forcing and warming increase across the SSPs demonstrates the importance of mitigating GHG emissions and controlling socioeconomic changes to reduce drought risk.

Exploring the driving forces of risk changes identifies hazard as the main driver for all drought extremity levels and future scenarios. For the increasing risk cases, about 50% of the increasing magnitude is attributed to the hazard and the remaining 50% is attributed to exposure and vulnerability, with a higher contribution from exposure. These findings underscore the significance of adopting a comprehensive approach to drought risk assessment that integrates all three elements of risk—hazard, exposure, and vulnerability. This approach can help inform the

development of more effective strategies for mitigating the impacts of drought and building resilience to its effects.

This study also underscores the significance of using a multivariate drought analysis approach that accounts for the collective changes in relevant variables for drought analysis in each sector. The use of a multivariate approach is particularly essential because hydroclimatic variables that are relevant to one drought type cannot be used as substitutes for each other¹⁷. For example, precipitation and runoff (or soil moisture) in Europe are projected to change in opposite directions^{3,49}, meaning that using a single hydrological variable as a proxy for drought analysis in different sectors can lead to erroneous conclusions. Therefore, it is crucial to consider the unique characteristics and needs of different sectors when taking a holistic approach to drought analysis. The multivariate drought indicator developed here based on copula functions can quantify the combined conditions of drought drivers for drought analysis. The advantage of this approach is that all drought drivers do not need to be in extreme conditions to account for drought impacts. By taking a comprehensive and integrative approach to drought analysis, decision-makers can have the necessary information to make informed choices and mitigate the impacts of drought on society and the environment.

The results of this study highlight the need for implementing drought risk mitigation and preparedness measures to address devastating direct and indirect effects that cascade through communities and ecosystems⁵⁰. These measures need to be implemented at various scales, including the sectoral level and the local community level, to adapt to the new normal conditions of reduced water availability and more frequent droughts⁵¹. If such measures are not taken, there is a risk of triggering environmental migration and water conflicts^{52,53}. At the local scale, community resilience efforts can help build capacity and promote social learning to cope with the negative impacts of drought⁵⁴.

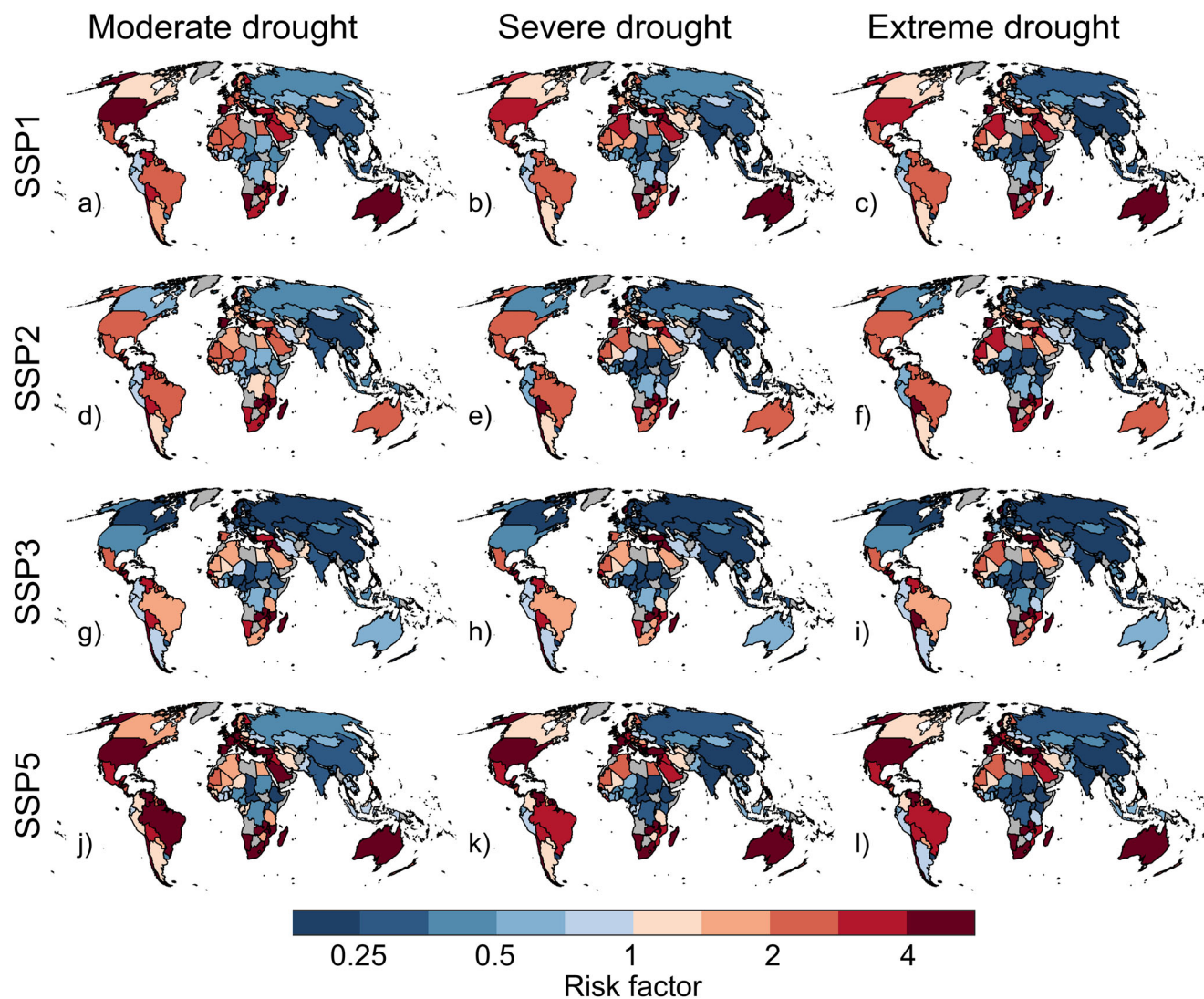


Fig. 4 Drought risk factor between the late 20th century and the late 21st century. Risk factors of moderate (a, d, g, j), severe (b, e, h, k) and extreme (c, f, i, l) droughts by the late 21st century (2070-2099) under different scenarios relative to the historical baseline period (1971-2000). Hazard (12-month drought), exposure, and vulnerability are normalized for the risk calculation. See Supplementary Fig. 11 for the drought risk factor derived from non-normalized hazard, exposure, and vulnerability.

Examples of such efforts include water and food conservation, developing drought-resistant crops and livestock varieties, and sustainable land and water management practices like water reuse, water harvesting, recharge, afforestation, and efficient use of water in agriculture (e.g., drip irrigation)⁵⁵⁻⁵⁷.

At the global scale, drought risk reduction initiatives aim to provide science-based information to support advocacy efforts and assess the potential efficacy of risk reduction solutions in regions most at risk⁸. Effective drought risk mitigation requires international coordination, particularly for countries that share transboundary water systems such as rivers, lakes, and aquifers⁵⁸. Such cooperation is essential to avoid conflicts during periods of drought^{59,60}. Our research shows that transboundary water resources are likely to become scarcer in many regions due to climate change, making cooperation even more critical for effective drought risk management. For example, the Orange-Senqu River basin in southern Africa, which encompasses Lesotho, South Africa, Namibia, and Botswana, is an area where transboundary water resources are expected to become increasingly scarce under future climate change (Fig. 1). Therefore, international cooperation is particularly crucial in this region to

ensure effective drought risk mitigation and reduce the risk of conflict.

Our study has shown that aggregated drought risk will disproportionately impact low- and lower-middle-income countries (e.g., in southern Africa and Southern America), where limited capital assets and human security make them particularly vulnerable. To address this, investing in disaster risk reduction for greater resilience is essential. The Sendai Framework for Disaster Risk Reduction, developed by the United Nations, outlines four priorities for action to help stakeholders effectively manage disaster risk⁶¹. These priorities include understanding disaster risk, strengthening disaster risk governance, investing in disaster risk reduction, and enhancing disaster preparedness to enable effective response and support recovery, rehabilitation, and reconstruction efforts with the aim of “Building Back Better”.

In addition to the measures mentioned above, shifting from hydropower and fossil fuels to wind and solar energy sources and raising awareness on drought hazards, exposure, and vulnerability are also crucial for effective drought risk mitigation^{62,63}. Specific examples of such measures include promoting solar-powered irrigation systems and educating farmers on sustainable

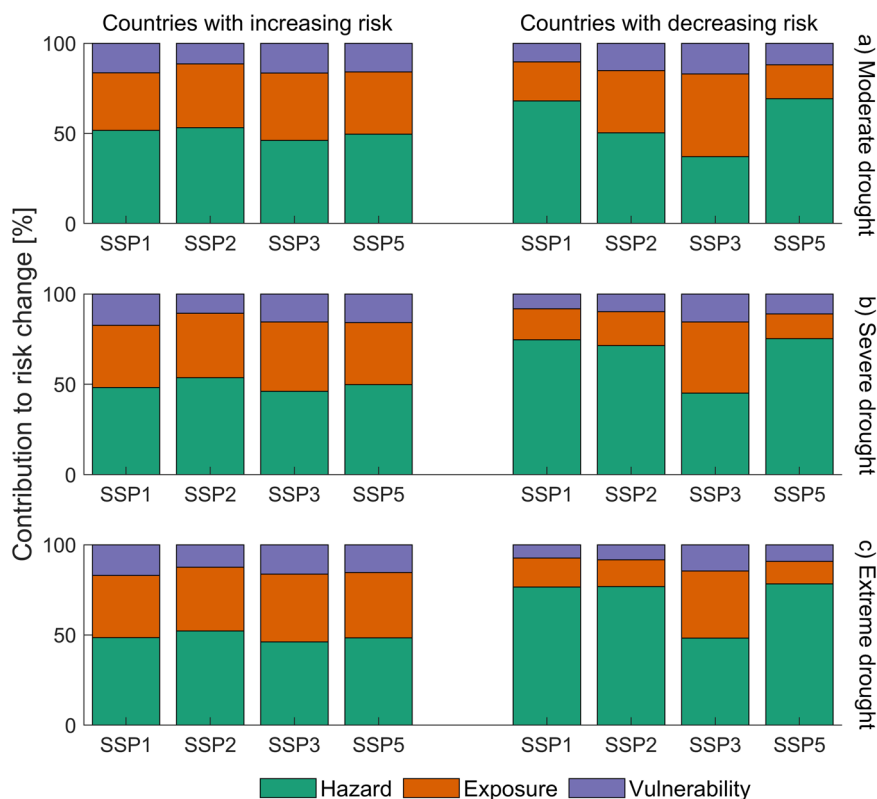


Fig. 5 Contribution of hazard, exposure, and vulnerability to the change in drought risk. The median contribution across countries with increasing and decreasing risk of moderate (a), severe (b), and extreme (c) droughts is shown. Hazard was calculated for a 12-month scale.

agricultural practices^{64,65}. By implementing these measures at various scales, we can better mitigate the impacts of drought and promote greater resilience in vulnerable communities and ecosystems.

Recommendations for future work. While this study represents a notable advancement in understanding global-scale drought risk, there is always room for improvement in methodological frameworks. Here are some recommendations for future work on improving the methodological frameworks of drought risk studies:

Hazard: It's important to consider the specific needs and characteristics of different regions and sectors when developing drought indicators. While precipitation, runoff, and soil moisture as commonly-used hydrological variables for drought analysis were employed in this study, they may not be sufficient for capturing the unique aspects of water availability in certain regions or sectors such as agriculture and nature/ecology. For example, in regions where water supply is heavily reliant on snowpack, reservoir storage, and/or hydraulic flow regulation, it may be important to include variables such as snow water equivalent, reservoir storage capacity, and hydraulic regulation strategy in drought indicators. Similarly, in regions where the withdrawal of surface and/or groundwater resources is important, information on this withdrawal may be critical for understanding the impact of drought on water availability.

Exposure and vulnerability: While the HDI is an indicator used for assessing vulnerability to various hazards, it may not fully capture the specific vulnerabilities to drought. Future studies may benefit from incorporating additional proxy indicators relevant to drought vulnerability. In addition, the HDI was developed at the national level, but there can be substantial variation in vulnerability to drought within a country, especially in large

countries. Developing the HDI at a smaller spatial scale, such as at the regional or local level, can provide more detailed and accurate information about the distribution of vulnerability to drought. This can help policymakers and practitioners to target interventions and resources to areas and communities that are most at risk, and to tailor their strategies to the specific needs and characteristics of different regions and populations. Furthermore, while the analysis in this study considers exposure of the entire population at each location, there may be differential vulnerabilities across populations based on age, socioeconomic status, and other factors.

Future studies could incorporate the above-mentioned recommendations to provide a more nuanced understanding of future drought risk. Despite these limitations, this study represents a significant step forward in global drought risk management by integrating future projections of population exposure, an indicator of socioeconomic vulnerability, and a multivariate drought indicator.

Methods

Data. To ensure comprehensive coverage of all three types of drought (meteorological, agricultural, and hydrological), the study utilized data on precipitation flux (both liquid and solid phases), total runoff (including drainage through the base of the soil model), and total soil moisture content (water in all phases summed over all soil layers). The data were obtained from 18 CMIP6 GCMs that provided information on these variables for historical simulations from 1971–2014 and four future tier 1 scenarios (SSP1-2.6, SSP2-4.5, SSP3-7.0, and SSP5-8.5) for the period 2015–2099 (Supplementary Table 1). It should be noted that SSP1-2.6, SSP2-4.5, and SSP5-8.5 are continuations of the previous RCP2.6, RCP4.5, and RCP8.5 scenarios, while SSP3-7.0 represents a new scenario with high-level emissions (Supplementary Note 1⁶⁶).

Hazard. The multivariate standardized drought index (MSDI) was developed for each grid cell of the CMIP6 GCMs, based on the joint distribution of precipitation, runoff, and soil moisture derived from copula functions. The MSDI is a trivariate index for a specific time scale of the variables (e.g., 1 month and 3 months) and is

expressed as:

$$H(x_1, x_2, x_3) = C(F_1(x_1), F_2(x_2), F_3(x_3)) = C(u_1, u_2, u_3) \quad (1)$$

where H is a three-dimensional distribution function of random variables x_1 , x_2 , and x_3 , C is a copula function, and u_1 , u_2 , and u_3 are variables produced by marginal distribution functions F_1 , F_2 , and F_3 , respectively⁶⁷. The marginal distributions were computed using the empirical Gringorten plotting position⁶⁸ to avoid making assumptions about distribution forms across the globe. The best-fit copula family was determined based on the Bayesian Information Criteria.

Because of the difficulty of constructing three-dimensional functions by copulas^{69,70}, we coupled two bivariate copulas to construct a three-dimensional function as:

$$C(u_1, u_2, u_3) = C_2(C_1(u_1, u_2), u_3) = p \quad (2)$$

where C_1 is the first bivariate copula function corresponding to variables u_1 and u_2 , C_2 is the second bivariate copula function corresponding to variables $C_1(u_1, u_2)$ and u_3 , and p is the joint probability. The C_1 and C_2 are the same type of copula function.

The MSDI was then computed based on the joint probability p (Eq. 2) as:

$$\text{MSDI} = \varphi^{-1}(p) \quad (3)$$

where φ is the standard normal distribution function¹⁰. The MSDI follows the drought classifications of the Standardized Precipitation Index (SPI⁷¹) (Supplementary Table 2).

The MSDI was calculated for an annual time scale (12 months), representing the anomalies of accumulated values for the given month and 11 previous months. The 12-month scale was found to be the best predictor for drought impacts across different sectors and regions⁷². This is the time scale of the globally most extreme drought events in the last decades⁷³. However, to check the sensitivity of the results to the time scale, the MSDI was also calculated for the 3-month scale. The anomalies were calculated for the whole period 1971–2099 as the baseline to ensure a more robust and reliable quantification of the standardized index⁷⁴. Driving the MSDI time series separately for historical and future periods to obtain climate change signals may lead to unrealistic results because normal conditions in the past will change under future climate change⁷⁵.

After computing MSDI, drought events were identified as every time the MSDI indicator falls below a given threshold. Similar to the widely accepted drought classifications based on the SPI, three thresholds of -1 , -1.5 , and -2 corresponding to the upper limits of moderate, severe, and extreme droughts were used in this study (Supplementary Table 2). The probability of occurrence of drought for historical (1971–2000) and future (2070–2099) periods was defined as the number of drought months over the total number of months in each period, and this was calculated for moderate, severe, and extreme droughts. The probability ratio was calculated as the ratio of the probability of occurrence of drought in the future period over that in the historical period. In total, the probability ratio at each pixel was determined for 216 combinations (18 GCMs \times 4 SSPs \times 3 drought extremity levels). The robustness of the probability ratio was assessed based on the consistency of the sign of the probability ratio among the CMIP6 ensemble members. A probability ratio is deemed robust when more than 72% of the models (13 out of the 18 GCMs) agree on its sign.

Exposure. To investigate the population exposure to drought, we utilized population density data with $0.5^\circ \times 0.5^\circ$ spatial resolution and annual temporal resolution for both the historical period (1971–2000) and the future period (2070–2099). The gridded population dataset, developed as part of the ISIMIP project (<https://www.isimip.org/gettingstarted/input-data-bias-adjustment/details/62/>), included historical population density from the HYDE3.2 database⁷⁶, and future population data derived from national decadal population projections based on SSP1, SSP2, SSP3, and SSP5, which were linearly interpolated to the annual scale³¹. We calculated the median population density of historical and future periods at each grid cell exposed to different probabilities of moderate, severe, and extreme drought at the corresponding grid cell (Fig. 3 and Supplementary Figs. 5, 6). Finally, we aggregated the gridded population density to the country level for risk analysis.

Vulnerability. We evaluated the vulnerability of different countries to drought using the Human Development Index (HDI). The HDI is a composite indicator of life expectancy, educational level, and income developed by the United Nations Development Program (UNDP). Life expectancy serves as a proxy for health, educational level corresponds to awareness and knowledge of hazard prevention, and income reflects the mitigation ability of individuals and governments. A historical vulnerability was assessed using HDI values for 2005, while projected HDI values³⁰ under SSP1, SSP2, SSP3, and SSP5 pathways for 2075 were used to estimate future vulnerability. As HDI values and risk have an inverse relationship (lower HDI values correspond to higher vulnerability), we used one minus HDI for the risk analysis.

Risk and its drivers. The risk of drought was defined as a multiplicative combination of hazard, exposure, and vulnerability. As these determinants have different units, they need to be normalized before the integration for risk analysis. Although

drought occurrence probability and HDI theoretically fall within the 0–1 range, the obtained values cover a far smaller range (e.g., 0.03–0.57 for the probability of extreme drought). In that case, normalizing only the population values will give a higher weight to the population exposure in the attribution analysis. To avoid such an error, drought occurrence probability and HDI were also normalized between 0.05 and 0.95, similar to the population exposure. The normalization range of 0.05–0.95 was chosen to prevent zero values for the risk components. The risk was calculated as

$$\text{Risk} = \text{hazard} \times \text{exposure} \times \text{vulnerability} = \text{MSDI}(p) \times \text{POP}_{\text{med}} \times (1 - \text{HDI}) \quad (4)$$

where POP_{med} is the median population for both the historical (1971–2000) and future (2070–2099) periods. The risk was determined for moderate, severe, and extreme drought events, where $\text{MSDI}(p)$ is the probability of MSDI-based droughts. Similar to the probability ratio of the drought hazard occurrence, the risk factor was calculated as the ratio of the drought risk in the future period over that in the historical period to quantify the expected future changes in drought risk.

To assess the drivers of risk changes, we decomposed the risk change into hazard, exposure, and vulnerability contributions using a sensitivity analysis. We calculated the contribution of each component by first calculating the risk using the other two components for both historical and future periods. Next, we calculated the change in the two-component risk between the historical and future periods. Finally, we determined the contribution as the absolute difference between the percentage change magnitudes derived from the two- and three-component risks. The percentage contribution for each component was computed as the ratio of the contribution of each component over the summation of the contributions of all three components.

Data availability

The CMIP6 soil moisture, runoff and precipitation data used in this study can be accessed online through the Earth System Grid Federation (ESGF) system (<https://esgf-node.llnl.gov/search/cmip6/>). The population data are available at the ISIMIP repository (<https://www.isimip.org/gettingstarted/input-data-bias-adjustment/>).

Code availability

The MATLAB code for drought characterization is available on request.

Received: 6 January 2023; Accepted: 5 May 2023;

Published online: 25 May 2023

References

1. WMO. *WMO Atlas of Mortality and Economic Losses from Weather, Climate and Water Extremes (1970–2019)*. WMO-No. 1267 (2021).
2. Tabari, H. & Willems, P. More prolonged droughts by the end of the century in the Middle East. *Environ. Res. Lett.* **13**, 104005 (2018).
3. Cook, B. I. et al. Twenty-first century drought projections in the CMIP6 forcing scenarios. *Earths Future* **8**, e2019EF001461 (2020).
4. Lange, S. et al. Projecting exposure to extreme climate impact events across six event categories and three spatial scales. *Earths Future* **11**, e2020EF001616 (2020).
5. HMNDP – High Level Meeting on National Drought Policies Towards More Drought Resilient Societies. Geneva, 11 – 15 March 2013. [online]. <http://www.wmo.int/pages/prog/wcp/drought/hmndp/index.php> (2013).
6. UN General Assembly (UNGA). A/RES/70/1 transforming our world: the 2030 agenda for sustainable development. *Resolut* **25**, 1–35 (2015).
7. Zhang, B., Wang, S. & Wang, Y. Copula-based convection-permitting projections of future changes in multivariate drought characteristics. *J. Geophys. Res. Atmos.* **124**, 7460–7483 (2019).
8. Ward, P. J. et al. Natural hazard risk assessments at the global scale. *Nat. Haz. Earth Syst. Sci.* **20**, 1069–1096 (2020).
9. Wanders, N., Loon, A. F. V., & Van Lanen, H. A. Frequently used drought indices reflect different drought conditions on global scale. *Hydrol. Earth Syst. Sci. Dis.* 1–16 (2017).
10. Hao, Z. & AghaKouchak, A. Multivariate standardized drought index: a parametric multi-index model. *Adv. Water Resour.* **57**, 12–18 (2013).
11. Berg, A., Sheffield, J. & Milly, P. C. Divergent surface and total soil moisture projections under global warming. *Geophys. Res. Lett.* **44**, 236–244 (2017).
12. Cook, B. I., Mankin, J. S. & Anchukaitis, K. J. Climate change and drought: from past to future. *Curr. Clim. Change Rep.* **4**, 164–179 (2018).
13. Knutti, R. & Sedláček, J. Robustness and uncertainties in the new CMIP5 climate model projections. *Nat. Clim. Change* **3**, 369–373 (2013).

14. Dai, A., Zhao, T. & Chen, J. Climate change and drought: a precipitation and evaporation perspective. *Curr. Clim. Change Rep.* **4**, 301–312 (2018).
15. Tabari, H., Hosseinzadehtalaei, P., Thiery, W. & Willems, P. Amplified drought and flood risk under future socioeconomic and climatic change. *Earths Future* **9**, e2021EF002295 (2021).
16. Mankin, J. S., Seager, R., Smerdon, J. E., Cook, B. I. & Williams, A. P. Mid-latitude freshwater availability reduced by projected vegetation responses to climate change. *Nat. Geosci.* **12**, 983–988 (2019).
17. Lawrence, J., Blackett, P. & Cradock-Henry, N. A. Cascading climate change impacts and implications. *Clim. Risk Manag.* **29**, 100234 (2020).
18. Nie, M. et al. Bayesian-based time-varying multivariate drought risk and its dynamics in a changing environment. *Catena* **204**, 105429 (2021).
19. Yang, X. et al. Development of a multi-GCMs Bayesian copula method for assessing multivariate drought risk under climate change: a case study of the Aral Sea basin. *Catena* **212**, 106048 (2022).
20. Nikraftar, Z., Mostafaie, A., Sadegh, M., Afkueieh, J. H. & Pradhan, B. Multi-type assessment of global droughts and teleconnections. *Weather Clim. Extremes* **34**, 100402 (2021).
21. Ji, Y. et al. Multivariate global agricultural drought frequency analysis using kernel density estimation. *Ecol. Eng.* **177**, 106550 (2022).
22. Liu, Y. & Chen, J. Future global socioeconomic risk to droughts based on estimates of hazard, exposure, and vulnerability in a changing climate. *Sci. Tot. Environ.* **751**, 142159 (2021).
23. Wang, D., Hejazi, M., Cai, X. & Valocchi, A. J. Climate change impact on meteorological, agricultural, and hydrological drought in central Illinois. *Water Resour. Res.* **47**, W09527 (2011).
24. Rajsekhar, D. & Gorelick, S. M. Increasing drought in Jordan: climate change and cascading Syrian land-use impacts on reducing transboundary flow. *Sci. Adv.* **3**, 1–16 (2017).
25. Li, Y., Ye, W., Wang, M. & Yan, X. Climate change and drought: a risk assessment of crop-yield impacts. *Clim. Res.* **39**, 31–46 (2009).
26. Smirnov, O. et al. The relative importance of climate change and population growth for exposure to future extreme droughts. *Clim. Change* **138**, 41–53 (2016).
27. Arnell, N. W., Lowe, J. A., Lloyd-Hughes, B. & Osborn, T. J. The impacts avoided with a 1.5 °C climate target: a global and regional assessment. *Clim. Change* **147**, 61–76 (2018).
28. Liu, W. et al. Global drought and severe drought-affected populations in 1.5 and 2 °C warmer worlds. *Earth Syst. Dyn.* **9**, 267–283 (2018).
29. Gu, L. et al. Projected increases in magnitude and socioeconomic exposure of global droughts in 1.5 and 2 °C warmer climates. *Hydrol. Earth Syst. Sci.* **24**, 451–472 (2020).
30. Pokhrel, Y. et al. Global terrestrial water storage and drought severity under climate change. *Nat. Clim. Change* **11**, 226–233 (2021).
31. Samir, K. C. & Lutz, W. Demographic scenarios by age, sex and education corresponding to the SSP narratives. *Popul. Environ.* **35**, 243–260 (2014).
32. Alfieri, L., Feyen, L., Dottori, F. & Bianchi, A. Ensemble flood risk assessment in Europe under high end climate scenarios. *Glob. Environ. Change* **35**, 199–212 (2015).
33. Jongman, B. et al. Declining vulnerability to river floods and the global benefits of adaptation. *Proc. Natl Acad. Sci. USA* **112**, E2271–E2280 (2015).
34. Russo, S. et al. Half a degree and rapid socioeconomic development matter for heatwave risk. *Nat. Commun.* **10**, 1–9 (2019).
35. Knorr, W., Arneth, A. & Jiang, L. Demographic controls of future global fire risk. *Nat. Clim. Change* **6**, 781–785 (2016).
36. Crespo Cuaresma, J. & Lutz, W. The demography of human development and climate change vulnerability: a projection exercise. *Vienna Yearb. Popul. Res.* **13**, 241–262 (2015).
37. Lavell, A. et al. *Climate change: new dimensions in disaster risk, exposure, vulnerability, and resilience Managing the Risks of Extreme Events and Disasters to Advance Climate Change Adaptation*. A Special Report of Working Groups I and II of the Intergovernmental Panel on Climate Change (IPCC) (eds Field, C. B. et al) 25–64 (Cambridge Univ. Press, 2012).
38. O'Neill, B. C. et al. A new scenario framework for climate change research: the concept of shared socioeconomic pathways. *Clim. Change* **122**, 387–400 (2014).
39. Dixon, J. A., Gibbon, D. P., & Gulliver, A. *Farming Systems and Poverty: Improving Farmers' Livelihoods in a Changing World* (FAO, 2001).
40. Andrijevic, M., Cuaresma, J. C., Muttarak, R. & Schlessner, C. F. Governance in socioeconomic pathways and its role for future adaptive capacity. *Nat. Sustain.* **3**, 35–41 (2020).
41. Kharin, V. V. et al. Risks from climate extremes change differently from 1.5 C to 2.0 C depending on rarity. *Earths Future* **6**, 704–715 (2018).
42. Tabari, H. Climate change impact on flood and extreme precipitation increases with water availability. *Sci. Rep.* **10**, 1–10 (2020).
43. Li, C. et al. Larger increases in more extreme local precipitation events as climate warms. *Geophys. Res. Lett.* **46**, 6885–6891 (2019).
44. Hosseinzadehtalaei, P., Tabari, H. & Willems, P. Climate change impact on short-duration extreme precipitation and intensity–duration–frequency curves over Europe. *J. Hydrol.* **590**, 125249 (2020).
45. Tabari, H. Extreme value analysis dilemma for climate change impact assessment on global flood and extreme precipitation. *J. Hydrol.* **593**, 125932 (2021).
46. Takakura, J. Y. et al. Dependence of economic impacts of climate change on anthropogenically directed pathways. *Nat. Clim. Change* **9**, 737–741 (2019).
47. Tebaldi, C. et al. Climate model projections from the scenario model intercomparison project (ScenarioMIP) of CMIP6. *Earth Syst. Dyn.* **12**, 253–293 (2021).
48. Scheff, J. & Frierson, D. M. Scaling potential evapotranspiration with greenhouse warming. *J. Clim.* **27**, 1539–1558 (2014).
49. Satoh, Y. et al. A quantitative evaluation of the issue of drought definition: a source of disagreement in future drought assessments. *Environ. Res. Lett.* **16**, 104001 (2021).
50. McGlade, J. et al. Global assessment report on disaster risk reduction 2019. UN Office for Disaster Risk Reduction (UNDRR). https://gar.undrr.org/sites/default/files/reports/2019-05/full_gar_report.pdf (2019).
51. Rötter, R. P., Carter, T. R., Olesen, J. E. & Porter, J. R. Crop–climate models need an overhaul. *Nat. Clim. Change* **1**, 175–177 (2011).
52. Myers, N. Environmental refugees: a growing phenomenon of the 21st century. *Philos. Trans. R. Soc. Lond. B Biol. Sci.* **357**, 609–613 (2002).
53. Hsiang, S. M., Burke, M. & Miguel, E. Quantifying the influence of climate on human conflict. *Science* **341**, 1235367 (2013).
54. Amirzadeh, M. & Barakpour, N. Strategies for building community resilience against slow-onset hazards. *Int. J. Disaster Risk Reduct.* **66**, 102599 (2021).
55. McCormick, P. et al. *Tackling Change: Future-proofing Water, Agriculture, and Food Security in an Era of Climate Uncertainty* (International Water Management Institute, 2013).
56. Ward, P. J. et al. The need to integrate flood and drought disaster risk reduction strategies. *Water Secur.* **11**, 100070 (2020b).
57. Haile, G. G. et al. Droughts in East Africa: causes, impacts and resilience. *Earth Sci. Rev.* **193**, 146–161 (2019).
58. Cooley, H. & Gleick, P. H. Climate-proofing transboundary water agreements. *Hydrol. Sci. J.* **56**, 711–718 (2011).
59. Battistello Espindola, I. & Ribeiro, W. C. Transboundary waters, conflicts and international cooperation-examples of the La Plata basin. *Water Int.* **45**, 329–346 (2020).
60. Vij, S., Warner, J. & Barua, A. Power in water diplomacy. *Water Int.* **45**, 249–253 (2020).
61. United Nations Office of Disaster Risk Reduction (UNISDR). Sendai framework for disaster risk reduction 2015–2030. In *Paper Presented at the Third UN World Conference, Sendai, Japan* (2015).
62. Kamil, P. A., Utaya, S. & Utomo, D. H. Improving disaster knowledge within high school students through geographic literacy. *Int. J. Disaster Risk Reduct.* **43**, 101411 (2020).
63. Marshall, T. M. Risk perception and safety culture: tools for improving the implementation of disaster risk reduction strategies. *Int. J. Disaster Risk Reduct.* **47**, 101557 (2020).
64. Partey, S. T., Zougmore, R. B., Ouédraogo, M. & Campbell, B. M. Developing climate-smart agriculture to face climate variability in West Africa: challenges and lessons learnt. *J. Clean. Prod.* **187**, 285–295 (2018).
65. Al-Saidi, M. & Lahham, N. Solar energy farming as a development innovation for vulnerable water basins. *Dev. Pract.* **29**, 619–634 (2019).
66. O'Neill, B. C. et al. The scenario model intercomparison project (ScenarioMIP) for CMIP6. *Geosci. Model Dev.* **9**, 3461–3482 (2016).
67. Tabari, H. & Willems, P. Trivariate analysis of changes in drought characteristics in the CMIP6 multimodel ensemble at global warming levels of 1.5°, 2°, and 3 °C. *J. Clim.* **35**, 5823–5837 (2022).
68. Gringorten, I. I. A plotting rule for extreme probability paper. *J. Geophys. Res.* **68**, 813–814 (1963).
69. Grimaldi, S. & Serinaldi, F. Asymmetric copula in multivariate flood frequency analysis. *Adv. Water Resour.* **29**, 1155–1167 (2006).
70. Kao, S. C. & Govindaraju, R. S. Trivariate statistical analysis of extreme rainfall events via the Plackett family of copulas. *Water Resour. Res.* **44**, W02415, (2008).
71. McKee, T. B., Doesken, N. J., & Kleist, J. The relationship of drought frequency and duration to time scales. In *Proceedings of the 8th Conference on Applied Climatology* 179–183 (American Meteorological Society, 1993).
72. Blauhut, V. et al. Estimating drought risk across Europe from reported drought impacts, drought indices, and vulnerability factors. *Hydrol. Earth Syst. Sci.* **20**, 2779–2800 (2016).
73. Sheffield, J. & Wood, E. F. *Drought: Past Problems and Future Scenarios* (Earthscan, 2011).
74. Wu, H., Hayes, M. J., Wilhite, D. A. & Svoboda, M. D. The effect of the length of record on the standardized precipitation index calculation. *Int. J. Climatol.* **25**, 505–520 (2005).

75. Spinoni, J. et al. Future global meteorological drought hot spots: a study based on CORDEX Data. *J. Clim.* **33**, 3635–3661 (2020).
76. Klein Goldewijk, K., Beusen, A., Doelman, J. & Stehfest, E. Anthropogenic land use estimates for the Holocene–HYDE 3.2. *Earth Syst. Sci. Data* **9**, 927–953 (2017).

Acknowledgements

We extend our sincere appreciation to Prof. Wolfgang Lutz from the University of Vienna and Prof. Jesus Crespo Cuaresma from the Vienna University of Economics and Business for generously providing us with the future projections of the Human Development Index. Our gratitude also goes to the CMIP6, population, and land use data providers. We acknowledge the support of two Research Foundation—Flanders (FWO) grants, 12P3219N and 12P3222N, which enabled us to conduct this research.

Author contributions

H.T. was responsible for the study design and statistical analyses, as well as the writing of the manuscript, which was reviewed and approved by P.W.

Competing interests

The authors declare no competing interests.

Additional information

Supplementary information The online version contains supplementary material available at <https://doi.org/10.1038/s43247-023-00840-3>.

Correspondence and requests for materials should be addressed to Hossein Tabari.

Peer review information *Communications Earth & Environment* thanks Ford Trenton and Marthe Wens for their contribution to the peer review of this work. Primary Handling Editors: Rahim Barzegar, Heike Langenberg.

Reprints and permission information is available at <http://www.nature.com/reprints>

Publisher's note Springer Nature remains neutral with regard to jurisdictional claims in published maps and institutional affiliations.



Open Access This article is licensed under a Creative Commons Attribution 4.0 International License, which permits use, sharing, adaptation, distribution and reproduction in any medium or format, as long as you give appropriate credit to the original author(s) and the source, provide a link to the Creative Commons license, and indicate if changes were made. The images or other third party material in this article are included in the article's Creative Commons license, unless indicated otherwise in a credit line to the material. If material is not included in the article's Creative Commons license and your intended use is not permitted by statutory regulation or exceeds the permitted use, you will need to obtain permission directly from the copyright holder. To view a copy of this license, visit <http://creativecommons.org/licenses/by/4.0/>.

© The Author(s) 2023